Computer-aided Investigation of Mechanical Properties for Integrated Casting and Rolling Processes Using Hybrid Numerical-analytical model of Mushy Steel deformation

Miroslaw Glowacki
Dept. of Applied Computer Science and Modelling
AGH-University of Science and Technology
A. Mickiewicza Av. 30, 30-059 Kraków, Poland
e-mail: glowacki@metal.agh.edu.pl

Marcin Hojny
Dept. of Applied Computer Science and Modelling
AGH-University of Science and Technology
A. Mickiewicza Av. 30, 30-059 Kraków, Poland
e-mail: mhojny@metal.agh.edu.pl

***Abstract*—The main subject of the current paper is investigation of yield stress for C45 grade steel as well as development of a new methodology of such investigation. The method requires high accuracy model of semi-solid steel deformation. Hence, it requires a dedicated hybrid analytical-numerical model of deformation of steel with variable density. The newly developed methodology allows to compute curves depending on both temperature and strain rate. The experimental work has been done in Institute for Ferrous Metallurgy in Gliwice Poland using Gleeble thermo-mechanical simulator with high temperature testing equipment. A number of compression and tension tests have been done in order to verify the predictive ability of both the developed model and new, modified testing methodology. The comparison between numerical and experimental results is the supplementary subject of the presented paper, as well. The developed methodology allows reliable numerical simulation of deformation of semi-solid steel samples and calculation of realistic flow curve parameters.**

Keywords-yield stress; semi-solid steel testing; extra-high deformation temperature; numerical analysis; inverse method

I. INTRODUCTION

Due to the global energy crisis in recent years, more and more new production technologies require energy preservation and environmental protection. The integrated casting and rolling technologies are newest efficient and very profitable ways of hot strip production. Only few companies all over the world are able to manage such processes. The technical staff of a plant located in Cremona, Italy is working on new methods of flat steel manufacturing for several years now. The ISP (Inline Strip Production) and AST (Arvedi Steel Technologies) technologies which are developed in Cremona are distinguished by very high rolling temperature. The main benefits of both the methods are related to very low rolling forces and favourable field of temperature. However, certain problems particular to such metal treatment arise. The central parts of slabs are mushy and the solidification is not yet finished while the deformation is in progress. This results in changes in material density and occurrence of characteristic temperatures having great influence on the plastic behaviour of the material [1, 2]. The nil strength temperature (NST), strength recovery temperature (SRT), nil ductility temperature (NDT) and ductility recovery temperature (DRT) have effect on steel plastic behaviour and limit plastic deformation. The nil strength temperature (NST) is the temperature level at which material strength drops to zero while the steel is being heated above the solidus temperature. Another temperature associated with NST is the strength recovery temperature (SRT). At this temperature the cooled material regains strength greater than 0.5 N/mm^2. Nil ductility temperature (NDT) represents the temperature at which the heated steel loses its ductility. The ductility recovery temperature (DRT) is the temperature at which the ductility of the material (characterised by reduction of area) reaches 5% while it is being cooled. Over this temperature the plastic deformation is not allowed at any stress tensor configuration.

The most important steel property having crucial influence on metal flow paths is the yield stress. In the literature of the past years, one can find papers regarding experimental results [3] and modelling [4] of non-ferrous metals. Both the mentioned contributions focus mainly on tixotrophy. The first results regarding steel deformation at extra high temperature were only presented in the past few years [5]. This stems from the fact that level of liquidus and solidus temperatures of steel is very high in comparison with non-ferrous metals. It causes serious experimental problems contrary to deformation tests for non-ferrous metals which are much easier. Rising abilities of thermo-mechanical simulators such as the Gleeble and development of new methods of identification of mechanical properties allow investigations leading to strain-stress relationships for semi-solid steels, as well. This problem became a subject of research done by authors of the presented paper for several years now. As a result a computer system supporting the investigation of mushy steel has been developed [6]. The current paper presents the modified methodology, which allows the calculation of the real stress-strain relationships for a wide range of temperatures and strain rate.

 ISBN: 978-1-61208-237-0

In the second section of the paper the modified methodology of stress-strain curves is described, the second one presents a mathematical model, in the last section an example results are presented. Finally, the main conclusions and future work are shortly described.

II. THE METHODOLOGY

Due to several serious experimental problems a special technique of testing was developed for temperatures higher than NDT. The deformation process has been divided into two main stages. The first one – a very small preliminary compression and the second one – the ultimate compression. The preliminary deformation is meant to eliminate clearances in the testing equipment. Well known Voce formula [6] has been applied to describe the yield stress functions. It takes account of a number of coefficients which are calculated using inverse analysis. This is the only acceptable method of interpretation of compression of semi-solid steel testing results. Due to strong temperature and strain inhomogeneity observed during compression of semi-solid samples the deformation causes significant barrelling of their central parts. Improvement of experimental methodology can help only to a small extent. Contrary to the old version of the method published in [6] the newly developed one allows the computation of curves depending on both temperature and strain rate. The tension tests has been replaced by compression ones and the Voce formula was replaced by more adequate equation. Fig. 1 schematically presents the modified methodology. More details concerning the experimental work were published in [7].

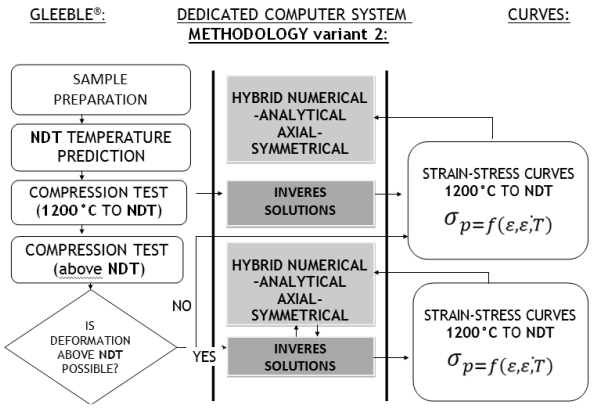

Figure 1. Flowchart of the integrated testing methodology of flow stress investigation of semi-solid steel.

The presented approach allows to compute realistic yield stress curves depending on strain, temperature and strain rate in temperature range from 1200°C to NDT and above. The objective function of the inverse analysis was defined as a square root error of discrepancies between calculated (F_c) and measured (F_m) loads at several subsequent steps of the compression process. The experimental values of the deformation forces were collected by the Gleeble equipment while the theoretical ones (F_c) were calculated with the help of a sophisticated solver facilitating accurate computation of strain, stress and temperature fields for materials with variable density. This solver is the least visible but the most powerful part of the computer aided testing system developed by the authors called Def_Semi_Solid (Fig. 2). The heart of the solver is based on a hybrid analytical-numerical mushy steel deformation model described in the next section.

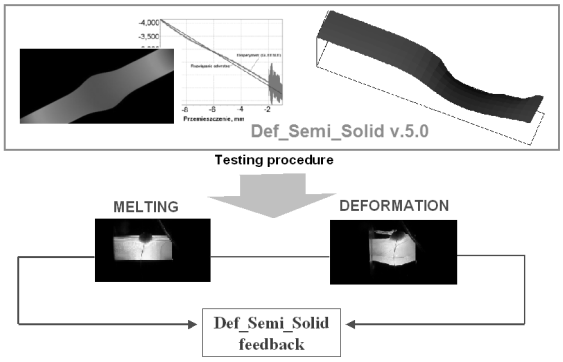

Figure 2. The Def_Semi_Solid system as a feedback unit with Gleeble simulator.

III. MATHEMATICAL MODEL

A mathematical model of the compression process has been developed using the theory of plastic flow. The principle of the upper assessment, calculus of variations, approximation theory, optimization and numerical methods for solving partial differential equations were used [8]. The following assumptions were established:

- Deformation and stress state are axial-symmetrical;
- Deformed material is isotropic but inhomogeneous;
- The material behaviour is rigid-plastic – the relationship between the stress tensor and strain rate tensor is calculated according to the Levy-Mises flow law [8], which is given as:

$$\sigma_{ij} - \frac{1}{3}\sigma_{kk}\delta_{ij} = \frac{2}{3}\frac{\sigma_p}{\dot{\varepsilon}_i}\dot{\varepsilon}_{ij} \quad (1)$$

Rigid-plastic model was selected due to its very good accuracy at the strain field during the hot deformation and sufficient correctness of calculated deviatoric part of the stress field. Moreover, the elastic part of each stress tensor component is very low at temperatures close to solidus line and can in practice be neglected in calculations of strain distribution. The limits for plastic metal behaviour are defined according to Huber-Mises-Hencky yield criterion:

$$\sigma_{ij}\sigma_{ij} = 2\left(\frac{\sigma_p}{\sqrt{3}}\right)^2 \quad (2)$$

In (1) and (2), σ_{ij} denotes the stress tensor components, σ_{kk} represents the mean stress, δ_{ij} is the Kronecker delta [8],

σ_p indicates the yield stress, $\dot{\varepsilon}_i$ is the effective strain rate, and $\dot{\varepsilon}_{ij}$ denotes strain rate tensor components. The components are given by an equation:

$$\dot{\varepsilon}_{ij} = \frac{1}{2}\left(\nabla_i v_j + \nabla_j v_i\right) \tag{3}$$

In cylindrical coordinate system $Or\theta z$ the solution is a vector velocity field defined by the distribution of three coordinates $\boldsymbol{v} = (v_r, v_\theta, v_z)$. The field is a result of optimization of a power functional, which can be written in general form as the sum of power necessary to run the main physical phenomena related to plastic deformation. Due to the axial-symmetry of the sample the circumferential component of the velocity field can be neglected and the functional is usually formulated as:

$$J[\boldsymbol{v}] = \dot{W} = \dot{W}_\sigma + \dot{W}_\lambda + \dot{W}_f \tag{4}$$

Component $\dot{W}_\sigma$ occurring in (4) represents the plastic deformation power, $\dot{W}_\lambda$ is the power which is a penalty for the departure from mass conservation condition, $\dot{W}_f$ denotes the friction power and $\boldsymbol{v} = (v_r, v_z)$ describes the reduced velocity field distribution.

Rigid-plastic formulation of metal deformation problem requires the condition of mass conservation in the deformation zone. In case of solids and liquids with a constant density, this condition can be simplified to the incompressibility condition. Such a condition is generally satisfied with sufficient accuracy during the optimization of functional (4). In most solutions a slight, but noticeable loss of volume is observed. The loss occurs because the incompressibility condition imposed on the solution is not completely satisfied in numerical form. It is negligible in case of traditional computer simulation of deformation processes although in some embodiments more accurate methods are used to restore the volume of metal subjected to the deformation. In contrast, in the presented case the density of semi-solid materials varies during the deformation process and these changes result in a physically significant change in the volume of a body having constant mass. The size of the volume loss due to numerical errors is comparable with changes caused by fluctuation in the density of the material.

A further problem specific to the variable density continuum is power $\dot{W}_\lambda$, which occurs in functional (4). It is used in most solutions and has a significant share of total power. Even when the iterative process approaches the end, this power component is still significant, especially if the convergence of the optimization procedures is insufficient. In case of discretization of the deformation area (e.g. using the finite element method) if one focuses solely on the $\dot{W}_\lambda$ a number of possible locally optimal solutions appear. They are related to a number of possible directions of movement of discretization nodes providing the volume preservation of the deformation zone. Each of these solutions creates a local optimum for $\dot{W}_\lambda$ power and thus for the entire functional (4). This makes it difficult to optimize because of lack of uniform direction of fall of total power which leads to global optimum. The material density fluctuation causes further optimization difficulties, resulting from additional replacement of incompressibility condition with a full condition of mass conservation.

The proposed solution requires high accuracy in ensuring the incompressibility condition for the solid material or mass conservation condition for the semi-solid areas. This stems from the fact that the errors resulting from the breach of these conditions can be treated as a volume change caused by the steel density variation in the semi-solid zone. High accuracy solution is required also due to large differences in yield stress for the individual subareas of the deformation zone. In the discussed temperature range they appear due to even slight fluctuations in temperature. In presented solution the second component of functional (4) is left out and mass conservation condition is given in analytical form constraining the radial (v_r) and longitudinal (v_z) velocity field components. The functional takes the following shape:

$$J[\boldsymbol{v}] = \dot{W}_\sigma + \dot{W}_t \tag{5}$$

In case of functional (5), the numerical optimisation procedure converges faster than the one for functional (4) due to the reduced number of velocity field parameters (only radial components are optimisation parameters) and the lack of numerical form of mass conservation condition. The accuracy of the proposed hybrid solution is higher also due to negligible volume loss caused by numerical errors, which is very important for materials with variable density.

As mentioned before, the solution of the problem is a velocity field in cylindrical coordinate system in axial-symmetrical state of deformation. Optimization of metal flow velocity field in the deformation zone of semi-variational problem requires the formulation according to equation (5). The radial velocity distribution $v_r(r, \theta, z)$ and the longitudinal one $v_z(r, \theta, z)$ are so complex that such wording in the global coordinate system poses considerable difficulties. These difficulties are the result of the mutual dependence of these velocities. Therefore the basic formulation will be written for the local cylindrical coordinate system $Or\theta z$ with a view to the future discretization of deformation area using one of the dedicated methods. In addition one will find that the deformation of cylindrical samples is characterized by axial symmetry. As demonstrated by experimental studies conducted using semi-solid samples the symmetry may be disturbed only as a result of unexpected leakage of liquid phase.

Such experiments, however, are regarded as unsuccessful and not subject to numerical analysis. Establishment of the axial symmetry, which except in cases of physical instability can be considered valid also for the process of compression or tensile test of semi-solid samples, allows one to simplify the model because of the identical strain distribution at any axial sample cross-section. Considerations will therefore be carried out in Orz coordinates for the sample cross-section using one of the planes containing the sample axis. Components of power functional given by (5) have been formulated in accordance with the general theory of

 ISBN: 978-1-61208-237-0

plasticity by relevant equations. The plastic power for the deformation zone having volume of V is given by the subsequent relation:

$$\dot{W}_\sigma = \int_V \sigma_i \dot{\varepsilon}_i \, dV \tag{6}$$

where σ_i is the effective stress and $\dot{\varepsilon}_i$ denotes the effective strain. The plastic deformation starts when the rising effective stress reaches yield stress limit σ_p ($\sigma_i = \sigma_p$) according to yield criterion given by equation (2). Effective strain occurring in (6) is calculated on the basis of the strain tensor components $\dot{\varepsilon}_{ij}$ according to following relationship:

$$\dot{\varepsilon}_i = \sqrt{\frac{2}{3}\dot{\varepsilon}_{ij}\dot{\varepsilon}_{ij}} \tag{7}$$

The components are given by (3). The second component of functional (5) is responding for friction. To compute friction power on the boundary S of area V a model given by the subsequent equation was used:

$$\dot{W}_t = \int_S m \frac{\sigma_p}{\sqrt{3}} \|\overline{\boldsymbol{v}}\| dS \tag{8}$$

In (8), m is the so called friction factor, which is usually experimentally selected and $\overline{\boldsymbol{v}}$ is a relative velocity vector of metal and tool $\overline{\boldsymbol{v}} = \boldsymbol{v} - \boldsymbol{v_t}$. In case of tensile test the samples are permanently fixed in jaws of a physical simulator and friction must not be taken into account. However, compression test requires sharing the friction power which is significant.

For the solid zones the incompressibility condition can be described by universal operator equation independently of the mechanical state of the deformation process:

$$\nabla \mathbf{v} = 0 \tag{9}$$

Because the semi-solid zone is characterized by density change due to still ongoing progress of steel solidification, the condition of incompressibility is inadequate to reflect changes and was replaced with the mass conservation condition, which describes the following modified operational equation:

$$\nabla \mathbf{v} - \frac{1}{\rho}\frac{\partial \rho}{\partial t} = 0 \tag{10}$$

The basis for the optimization of functional (5) is the velocity field determined by appropriate system of velocity functions in the concerned area. These functions are then the source of deformation field and other physical quantities affecting the power functional formulation. Obtaining an accurate real velocity field requires the use of velocity functions depending on a number of variational parameters. The functions should be flexible enough to map the field throughout the whole volume of the deformation zone. Analytical description of each component of the velocity field with a single function in the whole area of deformation is not preferred. This approach creates difficulties especially in areas not subjected to the deformation where the velocity function should remain constant. Therefore, the solution to the problem of semi-solid metal flow was based on a specific method.

In the case of deformation of axial-symmetrical bodies, the incompressibility condition is given by following differential equation:

$$\frac{\partial v_r}{\partial r} + \frac{v_r}{r} + \frac{\partial v_z}{\partial z} = 0 \tag{11}$$

For the semi-solid area, (11) is replaced by the mass conservation condition due to existing density changes. The longitudinal velocity has been calculated as an analytical function of radial velocity using this condition. In cylindrical coordinate system the condition has been described with an equation:

$$\frac{\partial v_r}{\partial r} + \frac{v_r}{r} + \frac{\partial v_z}{\partial z} - \frac{1}{\rho}\frac{\partial \rho}{\partial \tau} = 0 \tag{12}$$

Equation (11) is a special case of (12) and therefore the proposed solution will consider the dependence (12) as more general. In (12) ρ is the temporary material density and τ is the time variable. The proposed variational formulation makes the longitudinal velocity dependent on the radial one. Condition (12) allows for the calculation of $\partial v_z/\partial z$ derivative as a function of $\partial v_r/\partial r$ after analytical differentiation of radial velocity distribution function $v_r(r,z)$. Hence, the longitudinal velocity is calculated as a result of analytical integration according to following equation:

$$v_z = -\int \left(\frac{\partial v_r}{\partial r} + \frac{v_r}{r} - \frac{1}{\rho}\frac{\partial \rho}{\partial \tau}\right) dz \tag{13}$$

In this case, the velocity field depends only on one function – the radial velocity distribution.

Heat exchange between solid metal and environment, and its flow inside the metal is controlled by a number of factors. During phase transformation two additional phenomena have to be taken into account. Note that in the process of deformation of steel at temperature of liquid to solid phase transformation there are two sources of heat changes. On the one hand heat is generated due to the state transformation. On the other hand it is secreted as a result of plastic deformation. In addition, steel density variations also cause changes of body temperature.

Thermal solution has a major impact on simulation results, since the temperature has strong effect on remaining variables. This is especially evident if the specimen temperature is close to solidus line when the body consist of both solid and semi-solid regions. In such case the affected phenomena are: plastic flow of solid and mushy materials, stress evolution and density changes. The theoretical temperature field is a solution of Fourier-Kirchhoff equation with appropriate boundary conditions.

 ISBN: 978-1-61208-237-0

The most general form of the Fourier-Kirchhoff equation in any coordinate system can be written in operator form as follows:

$$\nabla^T(\mathbf{\Lambda}\,\nabla T) + Q = c_p\rho\left(\boldsymbol{v}^{\boldsymbol{T}}\nabla T + \frac{\partial T}{\partial \tau}\right) \qquad (14)$$

where T is the temperature distribution in the controlled volume and $\mathbf{\Lambda}$ denotes the symmetrical second order tensor called heat transformation tensor. In case of thermal inhomogeneity the whole tensor has to be considered. Q represents the rate of heat generation (or consumption) due to the phase transformation, due to plastic work done and due to electric current flow (resistance heating of the sample is usually applied). Finally c_p describes the specific heat, ρ the steel density, $\boldsymbol{v}$ the velocity vector of specimen particles and τ the elapsed time.

For axial-symmetrical case, (14) can be simplified. The following form of Fourier-Kirchhoff equations for isotropic, axially-symmetric heat flow was applied in the presented solution:

$$\lambda\left(\frac{\partial^2 T}{\partial r^2} + \frac{1}{r}\frac{\partial T}{\partial r} + \frac{\partial^2 T}{\partial z^2}\right) + Q = \rho c_p \frac{\partial T}{\partial \tau} \qquad (15)$$

Equation (15) needs to be solved with appropriate initial and boundary conditions. Combined Hankel's boundary conditions have been adopted for the presented model.

IV. EXAMPLE RESULTS

The experimental work was done in Institute for Ferrous Metallurgy in Gliwice, Poland using Gleeble thermo-mechanical simulator. The steel used for the experiments was the C45 grade steel having 0.45% of carbon content. In all cases, experiments were performed according to the following schedule:

- initial stage: sample preparation divided into several sub stages (e.g., thermocouple assembly); die selection, etc,
- stage 2: melting procedure,
- stage 3: deformation process.

It is good practice to test materials in isothermal conditions [9]. Unfortunately, this is not possible for semi-solid steel. Nevertheless, the condition should be as close to isothermal as possible due to the very high sensitivity of material rheology to even small variations of temperature. The basic reason for uneven temperature distribution inside the sample body on the Gleeble simulator is the contact with hot copper handles presented in Fig. 3.

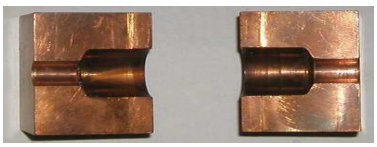

Figure 3. The short contact zone handles used in experiments (hot handle).

The estimated liquidus and solidus temperature levels of the investigated steel are: 1495°C and 1410°C, respectively. Thermal solution of the theoretical model has crucial influence on simulation results, since the temperature has strong effect on remaining parameters. The resistance sample heating and contact of the sample with cold cooper handles cause non-uniform distribution of temperature inside heated material, especially along the sample. The semi-solid conditions in central parts of the sample cause even greater temperature gradient due to latent heat of transformation. Such non-uniform temperature distribution is the source of significant differences in the microstructure and hence in material rheological properties.

During the experiments samples were heated to 1430°C and after maintaining at constant temperature were cooled down to the required deformation temperature. In case of heating the heat generated is usually not known because the Gleeble equipment uses an adaptive procedure for resistive heating controlled by temperature instead of current flow. Hence, the actual heat generated by current flow (in fact the rate of heat generation Q) has to be calculated using inverse procedure. In this case the objective function (F) was defined as a norm of discrepancies between calculated (T_c) and measured (T_m) temperatures at a checkpoint (steering thermocouple position: TC4 in Fig. 4) according to the following equation:

$$F(\mathrm{Q}) = \int_{\tau_0}^{\tau_i}[T_c(Q,r,z,T) - T_m(r,z,T)]d\tau \qquad (16)$$

where: where τ is the time variable, Q is the rate of heat generation.

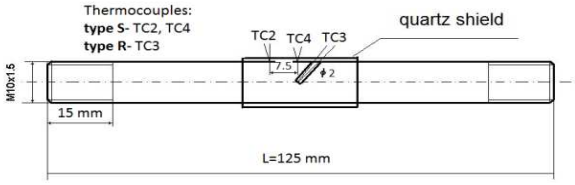

Figure 4. Samples used for the experiments. TC2, TC3 and TC4 thermocouples.

In the final stage of physical test, the temperature difference between core of the sample (TC3 thermocouple position) and its surface (TC4 thermocouple position) can be significant. In all cases the core temperature was higher than surface temperature. Differences between these two reach around 30°C for cold handle (handle with long contact zone) and about 40°C for hot handle. The results of numerical simulation are in agreement with experiments. Fig. 5 presents the temperature distributions in the cross section of sample tested at 1380°C right before deformation (variant with hot handle). One can observe major temperature gradient between die-sample contact surface. However, difference between experimental and theoretical core temperatures for hot handles was only 3°C (calculated core

temperature was equal to 1417°C and measured one was equal to 1420°C).

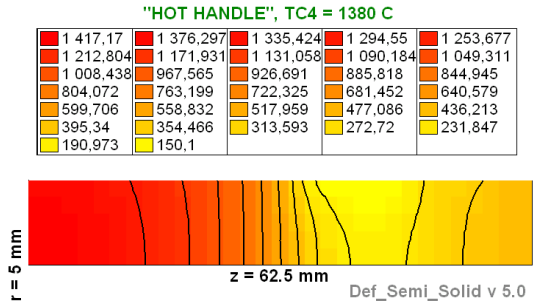

Figure 5. Distribution of temperature in the cross section of sample tested at temperature 1380°C right before deformation (variant with hot handle).

The micro and macrostructure of the tested samples were investigated as well. Fig. 6 shows microstructure right before deformation for both central and boundary regions of the heating zone. Microstructure of the cooled samples consists of pearlite (the darkest phase), bainite (grey phase mainly near the borders of grains) and the bright ferrite. This is a result of phase composition, wide melting zone and almost two times lower rate of cooling of central parts of the sample (in the case of hot handles).

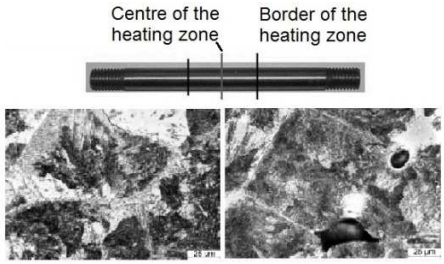

Figure 6. Microstructure of the central and boundary regions of sample right before deformation. Variant with cold handle. Magnification: 400x.

Fig. 7 shows macrostructure of the central part of cross-sections of samples right before deformation. Liquid phase particles were observed. Experimental and numerical results can be compared taking into consideration the temperature gradient within the sample. This shows that the mathematical model of resistance heating is consistent with the experimental data.

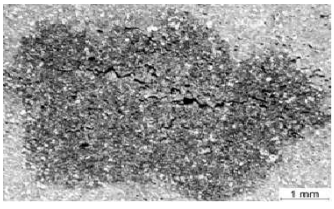

Figure 7. Macrostructure of the sample central part right before deformation. Variant with cold handle. Magnification: 10x.

Compression and tension tests were performed, according to the given methodology. During experiments die displacement, force and temperature changes in the deformation zone were recorded. The computer simulations were performed as well. All series of tests and computer simulations were done using long contact zone between samples and simulator jaws (cold handle). The deformation zone had the initial height of 62.5 mm. The sample diameter was 10 mm. The samples were melted at 1430°C, and then cooled to deformation temperature. During the tests each sample was subjected to 10 mm reduction of height. Results of each test were used for inverse analysis to compute yield stress curve parameters. Fig. 8 shows strain-stress curves at several strain rate levels for temperature 1300°C. The relationships were calculated using presented experimental methodology.

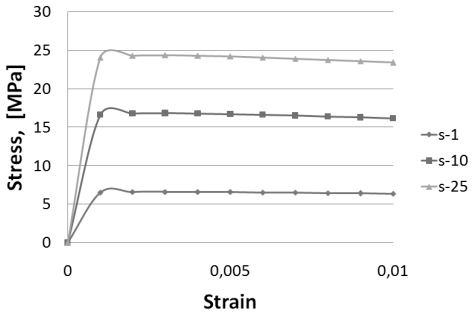

Figure 8. Stress-strain curves at several strain rate levels for temperature 1300°C.

Comparison between the calculated and measured loads are presented in Fig. 9, showing quite good agreement.

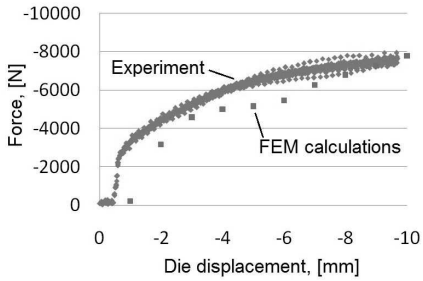

Figure 9. Comparison between measured and predicted loads at temperature 1380°C (new methodology).

Shape of a sample after experiment at 1300°C is presented in Fig. 10.

Figure 10. Example final shape of the sample after deformation at 1300oC.

Comparison between the measured and calculated maximal diameters of samples allow rough verification of

the developed computer aided experimental methodology. Results of such comparison are presented in Table 1. The table shows results for samples which have been subjected to deformation at several levels of temperature, i.e., 1300°C, 1350°C and 1380°C. Good agreement between the real diameter and its calculated value is observed. The relative mean square error between both the values is equal to 2.76%.

TABLE I. COMPARISION OF THE MEASURED AND CALCULATED MAXIMAL DIAMETERS OF SAMPLES DEFORMED AT DIFFERENT TEMPERATURE

Test	Experiment	Simulations
1300°C	15.3 mm	15.6 mm
1350°C	15.3 mm	15 mm
1380°C	17.8 mm	18.2 mm
Relative mean square error: 2.76%		

Fig. 11 compares measured loads with those computed using the methodology previously used by the authors. One can see that the mean square error in this case is significantly greater than its equivalent for the newly developed method.

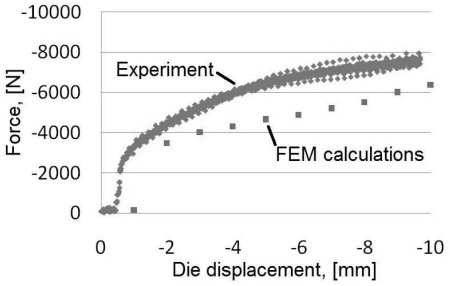

Figure 11. Comparison between measured and predicted loads at temperature 1380°C (old methodology).

The main reason for that is the lack of strain rate dependency of yield stress in the old model. The results obtained taking into account the strain rate as a parameter of the flow curve are more accurate for temperatures exceeding the NDT level.

V. CONCLUSION AND FUTURE WORK

The investigation reported in the current paper has shown, that temperature distribution inside the controlled semi-solid volume is strongly heterogeneous and non-uniform. Axial-symmetrical model does not take into account all the physical phenomena accompanying the deformation. Finally, the error of the predicted strain-stress curves can still be improved. The proposed solution of the presented problem is application of both fully three-dimensional solution and more adequate solidification model taking into consideration evolution of forming steel microstructure. Therefore, the study of multiscale modelling of mechanical properties is the main target of the future work. Contrary to the current model the new approach should allow to better capture the physical principles of semi-solid steel deformation in micro-scale. Additionally, the methodology should allow to transfer the characteristics of the material behaviour between the micro- and macro-scale. As a consequence the final results should be more precise and accurate. Modelling of deformation of steel samples at extra-high temperatures involves a number of issues. One of them is the difficulty of calculating of thermal and mechanical material properties. Another most important problem is the right interpretation of the results of compression tests that provide data for flow stress calculation. The presented testing methodology allows reliable numerical simulation of deformation of semi-solid steel samples and calculation of realistic flow curve parameters. The presented research was focused on mechanical properties of investigated semi-solid steel. Compression tests carried out for semi-solid materials could only be interpreted using inverse analysis. Temperature strain and strain rate as a parameters of the flow curve provide accurate results of computer simulation of semi-solid steel behaviour.

ACKNOWLEDGMENT

The work has been supported by the Polish Ministry of Science and Higher Education Grant N N508 585539

REFERENCES

[1] D. Senk, F. Hagemann, B. Hammer, and R. Kopp, “Umformen und Kühlen von direkt gegossenem,” Stahlband, Stahl und Eisen, vol. 120, 2000, pp. 65-69.

[2] H.G. Suzuki and S. Nishimura, “Physical simulation of the continuous casting of steels,” Proceedings of Physical Simulation of Welding, Hot Forming and Continuous Casting, Canmet Canada, May 2-4, 1988, pp. 166-191.

[3] R. Kopp, J. Choi, and D. Neudenberger, "Simple compression test and simulation of an Sn–15% Pb alloy in the semi-solid state," J. Mater. Proc. Technol.,vol. 135, 2003, pp. 317-323, doi: 10.1016/S0924-0136(02)00863-4.

[4] M. Modigell, L. Pape, and M. Hufschmidt,"The Rheological Behaviour of Metallic Suspensions," Steel Research Int., vol. 75, 2004, pp. 506–512.

[5] Y.L. Jing, S. Sumio, and Y. Jun, "Microstructural evolution and flow stress of semi-solid type 304 stainless steel," J. Mater. Proc. Technol., vol. 161, 2005, pp. 396–406, doi: 10.1016/j.jmatprotec.2004.07.063.

[6] M. Hojny and M. Glowacki," Computer modelling of deformation of steel samples with mushy zone," Steel Research Int., vol. 79, 2008, pp. 868-874. doi: 10.1007/1-4020-5370-3_537

[7] M. Hojny and M. Glowacki, "Modeling of strain-stress relationship for carbon steel deformed at temperature exceeding hot rolling range," Journal of Engineering Materials and Technology, vol. 133, 2011, pp. 021008.1-021008.7, doi: 10.1115/1.4003106.

[8] Z. Malinowski and R.Szyndler, “Axial transformation method in the analysis of the axisymmetrical plastic-flow,” Steel Research Int., vol. 58, 1987, pp. 503–507.

[9] M. Hojny and M. Glowacki, "The methodology of strain – stress curves determination for steel in semi-solid state," Archives of Metallurgy and Materials, vol. 54, 2009, pp. 475–483.

[10] M. Hojny and M. Glowacki, "The physical and computer modeling of plastic deformation of low carbon steel in semi-solid state," Journal of Engineering Materials and Technology, vol. 131, 2009, pp. 041003.1-041003.7, doi: 10.1115/1.3184034.

 ISBN: 978-1-61208-237-0